

# Comparative analysis of computational approaches for predicting Transthyretin transcription activators and human dopamine D1 receptor antagonists.

Mariya L. Ivanova\*, a, [ORCID](#), Nicola Russo, a, [ORCID](#) and Konstantin Nikolic, a, [ORCID](#)

Author affiliations:

\* Corresponding author [mariya.ivanova@uwl.ac.uk](mailto:mariya.ivanova@uwl.ac.uk)

a School of Computing and Engineering, University of West London, London, UK

## Abstract

The study expands the application of scikit-learn-based machine learning (ML) to the prediction of small biomolecule functionalities based on Carbon 13 isotope ( $^{13}\text{C}$ ) NMR spectroscopy data derived from Simplified Molecular Input Line Entry System (SMILES) notations. The methodology previously demonstrated by predicting dopamine D1 receptor antagonists was upgraded with addition of new molecular features derived from the PubChem database. The enhanced ML model obtained 75.8% Accuracy, 84.2% Precision, 63.6% Recall, 72.5% F1-score, 75.8 % ROC, when is trained by 25,532 samples and tested by 5,466 samples. To evaluate the applicability of the methodology for a variety of case studies, a comparison was conducted between the prediction capabilities of the ML models based on the human dopamine D1 receptor antagonists and on the neuronal Transthyretin (TTR) transcription activators. Since the TTR bioassay did not contain the needed for the comparison number of samples, the results were obtained hypothetically. Gradient Boosting classifier was the optimal model for TTR transcription activators achieving hypothetical 67.4% Accuracy, 74.0% Precision, 53.5% Recall, 62.1% F1-score, 67.4 % ROC, if it would be trained with 25,532 samples and tested with 5,466 samples. Beyond the main study, the CID\_SID ML model that can predict if a small biomolecule has TTR transcription activation capabilities based solely on its PubChem CID and SID achieved 81.5% Accuracy, 94.6% Precision, 66.8% Recall, 78.3% F1-score, 81.5 % ROC.

Keywords: neuronal TTR, machine learning, scikit-learn, DNN, PyTorch, Optuna,  $^{13}\text{C}$  NMR spectroscopy, IUPAC names-based ML model, CID\_SID ML model.

## Introduction

Nuclear Magnetic Resonance (NMR) Spectroscopy has been considered as one of the most powerful and informative techniques currently available for small biomolecule analysis (1). It provides detailed information about the arrangement of atoms within a molecule; identification of functional groups; three-dimensional arrangement of atoms in space; dynamics and interaction with other molecules; quantitative analyses (2). Enabling computers to learn from data through analysis and eliminating explicit programming, ML has been applied to data obtained via NMR spectroscopy such as employing message passing neural networks (MPNNs) to predict  $^{13}\text{C}$  NMR chemical shifts in small molecules (3); decreasing the ML errors of the NMR spectroscopy chemical shift predictions by using Deuterated chloroform (4); Computational structural elucidation aided by NMR spectroscopy and machine learning techniques (5); combining AlphaFold and chemical shift prediction in a deep learning model for faster protein NMR assignment (6); built from over 8,300 carbon atoms in diverse environments and without limitations on molecular complexity, a general-case neural network model was created for predicting (estimating)  $^{13}\text{C}$  NMR spectra (7).

Beyond ML, a range of computational methods listed below have been employed to predict NMR (8, 9) such as:

- (i) Computational "ab initio" techniques, meaning they operate "from first principles," determine a system's properties using only fundamental laws, in contrast to methods relying on empirical data. One such application is the development of a  $^{13}\text{C}$  NMR chemical shift prediction procedure for small molecule structure elucidation, which employed gauge invariant atomic orbitals with density functional theory and incorporated empirical systematic error correction terms (10).
- (ii) Additive increment-based approaches represent the initial methods for predicting chemical shifts where the core atomic shift has been subsequently modified by positive or negative contributions from attached substituents. Such rules, for instance, have been implemented in the CASPER program (11) to predict  $^{13}\text{C}$ ,  $^1\text{H}$ , and  $^{15}\text{N}$  shifts of polysaccharides.
- (iii) Hierarchical Organization of Spherical Environments (HOSE) code characterizes an atom's molecular environment by iteratively describing concentric spheres of neighbouring atoms. Essentially, this approach operates as a nearest neighbour search, where the HOSE code serves as the metric for defining structural similarity (9)

The online tool NMRDB (12) employed in the study to convert SMILES into  $^{13}\text{C}$  NMR spectroscopy data has been based on HOSE code and databases of existing NMR spectra and chemical structures reviewed by a board of reviewers (13). Recognizing that NMRDB-derived information represents a first approximation comparing to experimental data, its employment was sufficient for the demonstration of the proposed methodology idea within the current and previous studies.

The presented research had to solve two tasks: first, to assess the applicability of a pre-existing methodology (14) to a different case study; and second, to determine how the inclusion of molecular features would affect the accuracy of the investigated machine learning model. The existing methodology was an ML approach based on NMR spectroscopy data derived from SMILES notations, demonstrated by the case study on human dopamine D1 receptor antagonists, PubChem AID 504652 (15), which data was provide by PubChem, the world's largest database for freely available chemical information (16). The core idea of the existing ML approach was to leverage the relationship between a small biomolecule's carbon skeleton and the information provided by  $^{13}\text{C}$  NMR spectroscopy. The NMR spectrum, with its peaks indicates atomic bonds and ligands and elucidates of the molecular environment of the carbon atoms. This data was numerically encoded for machine learning, enabling its association with labels. So, it was anticipated and respectively demonstrated that  $^{13}\text{C}$  NMR spectroscopy could effectively contribute to the ML-based prediction of small biomolecule functionality.

The new case study, PubChem AID 1117267 bioassay (17) used for the comparison was also provided by PubChem. It was focused on TTR transcription activators containing 91,943 samples, 1,155 of which were defined as TTR activators. Data was obtained by High-throughput screening (HTS) which is an automated method in drug discovery and toxicology that rapidly tests vast compound libraries for biological activity using robotics and automated systems for parallel processing and analysis. The bioassay's aim has been conducted to identify and discover small biomolecules activating neuronal TTR transcription. Compounds

are tested in concentration of 16.7  $\mu$ M. For more information about the screening protocol, please refer to the bioassay documentation [17].

The protein TTR was called “the servant of many masters”. The primary functions of TTR are the transport of thyroid hormones and retinol through the blood stream and cerebrospinal fluid (18). However, its stability is critical, and misfolding can lead to amyloid disease, causing amyloidosis of nerves, ligaments, heart and arterioles (19) that could lead to polyneuropathy where multiple peripheral nerves become damaged (20), and/or cardiomyopathy affecting the heart muscles (21). Additionally, TTR has been reported to play an independent neuroprotective role in both the peripheral and central nervous systems, contributing to nerve function and repair (22, 23, 24). Using TTR Knockout mouse (25) it has been found out that the absence of transthyretin leads to increased levels of neuropeptide Y (NPY) in the brain and peripheral nervous system. Despite the need for additional research to fully elucidate the specific effects in TTR knockout mice, the study confirmed the presence of alterations in feeding behaviour, anxiety levels, stress responses, metabolic parameters, and potential changes in nerve function and repair (26).

So, overall, the protein TTR is an object of research for many scientists and clinicians due to its crucial roles in the body and its association with a significant and debilitating group of diseases known as transthyretin amyloidosis (ATTR).

Regarding the second objective of the presented research, which expanded the study beyond the comparison, molecular features obtained from PubChem were added to the NMR spectroscopy data to explore their influence on the ML models. Similar approach which has improved the MLmodel has been performed in studies regarding G9a (27, 28). These molecular features were, as follows:

- (i) Rotatable Bond Count (RBC) is determined by counting the single bonds that are not part of a ring and connect two non-hydrogen atoms that are also not at the end of a chain.
- (ii) Hydrogen Bond Acceptor Count (HDAC) refers to the number of hydrogen bond acceptors present in the given small biomolecule.
- (iii) Hydrogen Bond Donor Count (HBDC) refers to the number of hydrogen bond donors present in the given small biomolecule.
- (iv) Topological Polar Surface Area is computed as the surface sum over polar atoms in the molecule (29)
- (v) XLogP3 (XL) represents a predicted octanol-water partition coefficient (30).
- (vi) Molecular Weight (MW) is defined as the sum of the mass of all constituent atoms (31).

Furthermore, two additional ML applications were developed for researchers interested in TTR transcription activators. The first ML approach utilized an existing methodology (32) demonstrated on a case study focused on TDP1 inhibitors. The data encoded in the names that have been created according the International Union of Pure and Applied Chemistry (IUPAC) nomenclature (33) has been leveraged to generate a ranked list of functional groups based on their impact on the explored functionality of the small biomolecule. Subsequently these functional groups were analysed based on the proportion between their participating in the active and inactive samples. The functional groups that were a part only from the active samples` content were considered for the hypothesis that the presence of these functional groups carry the potential of TTR transcription activators. This ML approach

has the potential to contribute to the early stage of drug discovery giving probability for side effect with respect to TTR transcription activators. Given the concept of the article to compare the computational approaches applied for TTR and D1, the IUPAC based ML model was developed for D1 as well

The second ML approach aimed to predict whether a small biomolecule, initially designed for another purpose, could also function as a TTR transcription activator. This ML prediction was based exclusively on PubChem CID and SID data of the small biomolecule, using the methodology (34) that has previously demonstrated success in predicting the case studies related to CHOP inhibitors, dopamine D1 receptor antagonist, dopamine D3 receptor antagonist, TDP1 inhibitors, M1 muscarinic receptor antagonists, Rab 9 promoter activators and G9a enzyme inhibitors. While identifiers are generally not used in ML, PubChem identifiers can be an exception. This is because their generation process employs an algorithm that considers the structure and similarity between substances and compounds (35). For more details, please refer to the parent study (34).

Last, but not least, since the ML model of interest was classification, i.e. heavily dependent on the balance between the classes, the severe imbalance between the active and inactive biomolecules in the TTR bioassay dataset was handled through three steps. One of these steps incorporated PubChem AID 1996 bioassay focused on water solubility of small biomolecule (36), whose dataset was used as a sieve for the reduction of the small biomolecule without considering the level of aqua solubility of the samples.

## Methodology

The methodology followed whose applicability exploration was the aim of the research. For this purpose, the CID, SMILES notations and labels were extracted from the dataset of the PubChem AID 1117267 bioassay with 91,909 rows with small biomolecules and 9 columns with features describing these molecules. The samples detected as a TTR transcription activators were 1,155, called Active and 90,755 detected as Inactive compounds. The severe disbalance between the active and inactive compounds was initially decreased by merging the dataset of bioassay AID 1117267 with the dataset of the PubChem AID 1996 bioassay. Since the latter contained 57,856 samples of small biomolecule, this margin of both datasets played a role of a sieve reducing the number of the inactive compounds. Further, after shuffling of the inactive compounds only each eight samples of them were kept. The reduced inactive compounds, 2,023 samples, were then concatenated with all active compounds, i.e. 1,155 samples from the PubChem AID 1117267 bioassay dataset and the final dataset with 3,177 samples in total was obtained. Further, the SMILES notations of the resulting dataset were converted into numerical spectroscopy data employing the online tool NMRDB that has been designed for this purpose. The process requested each SMILES to be uploaded on the website where the NMRDB tool will generate <sup>13</sup>C NMR spectroscopy prediction, which was used to obtain the necessary for the ML data. The scale of the chemical shifts, i.e. the ppm, started from 0 and reached beyond 200. The scale was divided by natural numbers which defined subranges. These subranges were used as a feature and generated the columns in the data frame. The presence of a peak or peaks in each range were counted and placed as a value for the corresponded subrange of the relevant small biomolecule. Once all SMILES notations were converted to <sup>13</sup>C NMR spectroscopy data, the dataset was merged with the labels based on the SMILES notations. By this way since the canonical SMILES are unique was avoided misconnection between isomers.

To ensure the reliability of the evaluation, equal number of samples from each class were extracted and the testing set created. The remaining samples were balanced with oversampling. Although SMOTE is the technique that is generally recommended for balancing of data because it is expected to reduce overfitting and improve generalization, simulations for this study showed that Random Over Sampler was more effective. This involved increasing the minority class size to match the majority class by duplicating minority class samples. The balanced dataset was used for ML training with the RFC, DTC, GBC, and SVC estimators provided by the scikit learn ML library. The results of prediction were evaluated by the classification metrics which are based on the four possible scenarios: true positive (TP) and true negative (TN) where the prediction correspond to the actual values and false positive (FP) and false negative (FN) where they do not. So, the evaluation was done based on the metrics:

- (i) Accuracy – the total of correct prediction to the total of all predictions.
- (ii) Precision – true positive out of the total of all positive predictions.
- (iii) Recall – true positive out of all positive instances giving the sensitivity of the ML model
- (iv) F-1 score – indicates the balance between precision and recall
- (v) ROC (Receiver Operating Characteristic) shows the true positive against the false positive when the threshold varies.

The comparison of the results ranked the most optimal estimator for the case. The chosen ML model was scrutinised for overfitting tracing for the deviation between training and testing accuracy to be smaller than 5%.

To ensure the fairness in comparison between two cases, data set used for the ML model based on human dopamine D1 receptor antagonist data was reduced to the same number of active and inactive small biomolecules used in the TTR transcription activators prediction. Then the difference between the accuracy of ML based on the reduced D1 receptor antagonist dataset and the dataset used in the previous study was used for calculation how much the accuracy has been grown due to increase of the dataset samples. It was hypothesised that the existence of the same number of samples for the TTR case would increase the accuracy of the ML model with the same percentage.

ML with the enriched dataset was performed with the same manner explained above for the dopamine D1 receptor antagonist and for TTR transcription activators.

During the development of the prior study (14), which demonstrated the prediction of human dopamine D1 receptor antagonists, it was observed that the model was depended on the number of samples. To ensure a fair comparison in the current study, ML based on dopamine D1 receptor antagonists was conducting, using the same number of samples as the ML prediction of TTR transcription activators. Moreover, in the current study the molecular features were added to both the reduced dataset and the entire dataset for dopamine D1 receptor antagonists. The former was used for the purpose of comparison, and the latter was used to explore the effect that the molecular features caused on the accuracy in general.

Given the unique names which the IUPAC nomenclature provides, data obtained from IUPAC names was utilized for both classification ML predicting a small biomolecules` functionality and hierarchical ranking of the functional groups of these small biomolecule based on the influence these functional groups have on the considered small biomolecule functionality (32). For this purpose, the IUPAC names of the compounds from the bioassays focused on



dopamine D1 receptor antagonists and TTR transcription activators were parsed to single words equal or bigger than four letters. Each one of these words was used to create a column in a data frame and values in these columns corresponded to the this if there is or not such functional group in the small biomolecule. From this data frame, the functional groups that are part of the content of small biomolecules that that are only active were extracted in a descendent order. The hypothesis is that such a functional group has the strongest effect regardless of the considered functionality. This information can be used for potential side effects of a small biomolecule containing such a functional group. To increase the probability of predicting such influence, the <sup>13</sup>C NMR spectroscopy chemical shift can be used for comparison and draw conclusion based on similarity between the investigated compound and the explored small biomolecule.

## Results and discussion

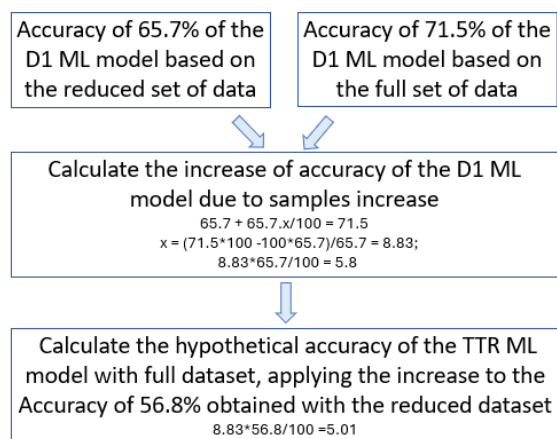
The results of comparison of the ML models are summarised in Table 1, providing connection with the relevant table or figure in the supplementary material.

Leveraging the methodology outlined above, the initial collection of inactive compounds from the TTR bioassay was narrowed down to 2,023 small biomolecules. Combining this reduced set of inactive samples with the full set of 1154 active compounds resulted in a data set with a total of 3177 rows and 209 columns. From this dataset a set of 340 samples per class was extracted for testing. The rest of the samples, after balancing the label proportion with SMOTE, were allocated for training. As a result of this, the ML models were trained with 2497 samples and tested with 680 samples. From the classifiers listed above, GBC was the optimal estimator, achieving 56.8% Accuracy, 59.2% Precision, 43.5% Recall, 50.2% F1-score, 56.8 % ROC (Table ESM1) and a five-fold cross-validation score of 0.651 with 0,02 standard deviation (Table ESM2). The deviation between the ML model performance and the cross validation implied overfitting, which was confirmed by comparing the train and test accuracies (Figure ESM1). Applying PCA slightly improved the Accuracy to 58.4%, ROC to 58.4 and Precision to 65.4%. However, the low Recall of 35.3% decreased the F1-score to 46.1% F1-score, which was an indicator for increment of the bias of the ML model towards the majority class, i.e. the inactive compounds, and thus the ML model can miss crucial instances of the minority class, i.e. the active compounds. (Table ESM3). The increased five-fold cross-validation score of 0.745 with 0,04 standard deviation (Table ESM4) compared to the single ML model accuracy suggested that the ML model was overfitted, which was confirmed tracing the deviation between train and test accuracy (Figure ESM2).

Regarding the dopamine D1 case, after the rows were reduced to correspond to the TTR dataset, ML was performed in the same manner as it was done for TTR case. The optimal estimator was SVM, obtaining 65.7 % Accuracy, 70.3% Precision, 54.4 % Recall, 61.4% F1-score, 65.7 % ROC (Table ESM5) and five-fold cross validation score of 0.775 with 0.02 standard deviation (Table ESM6). Expectedly, the ML model was overfitted (Figure 3). However, since the ML model based on full set of the available data for the dopamine D1 receptor antagonist was not overfitted [see the original research ([14](#))] it was hypothesised that the increase of the samples of the TTR case to the same amount of samples used in the dopamine D1 receptor case , i.e. 10,542 active and 46,496 inactive compounds, would improve the TTR ML model with the same percentage as the accuracy of the dopamine D1 ML model. The percentage of improvement of the ML model based on the increase of the samples number was calculated as follow: the accuracy of the ML model with reduced rows

plus the accuracy of the ML model with reduced rows multiplied by the unknown percentage should be equal to the accuracy of the ML model with non-reduced rows (Table 2). The increase with 5.8 in the accuracy of the ML model due to increase of the number of samples was 8.85%. So, it was hypothesised that the increase the number of samples for TTR case to the level of samples for the D1 case, i.e. 57,038 compounds would increase the accuracy of the ML model that predicts TTR transcription activators to 61.82%. Unlike the TTR case, the dimensionality reduction in the dopamine D1 receptor case did not improve the ML model (Table ESM7, Table ESM8, Figure ESM4)

The addition of above-mentioned molecular features to the  $^{13}\text{C}$  NMR data improved the ML models performance. Regarding the TTR dataset with 3177 samples, merging it with the molecular data led to decrease of the dataset to 3,041 samples (1,948 inactive and 1,093 active compounds). The optimal ML model for this case was GBC achieving 67.1% Accuracy, 74.0% Precision, 52.6% Recall, 61.5% F1-score, 67.1 % ROC (Table ESM9) and a five-fold cross-validation score of 0.693 with 0.02 standard deviation (Table ESM10). In order to meet the condition for equal samples between the dopamine D1 receptor antagonist and TTR transcription activator case studies, 1,948 inactive and 1,093 active compounds were extracted for the reduced dopamine D1 receptor dataset. In this case, the Accuracy of ML model increased to 76.2%, Precision to 85.0%, Recall to 63.5%, F1-score to 72.7% and ROC to 76.2% (Table 17) and 0.783 five-fold cross-validation score with 0.005 standard deviation (Table ESM18). Tracing the deviation between the train and test accuracies of these two ML models showed that the models were overfitted (Figure ESM5, Figure ESM6). The hyperparameter tuning with Optuna, with 10 studies for the former case and 5 studies for the latter one did not provide improvements. The dimensionality reduction did not improve the performance of the ML models (Table ESM12, Table ESM13, Table ESM14, Table ESM15)



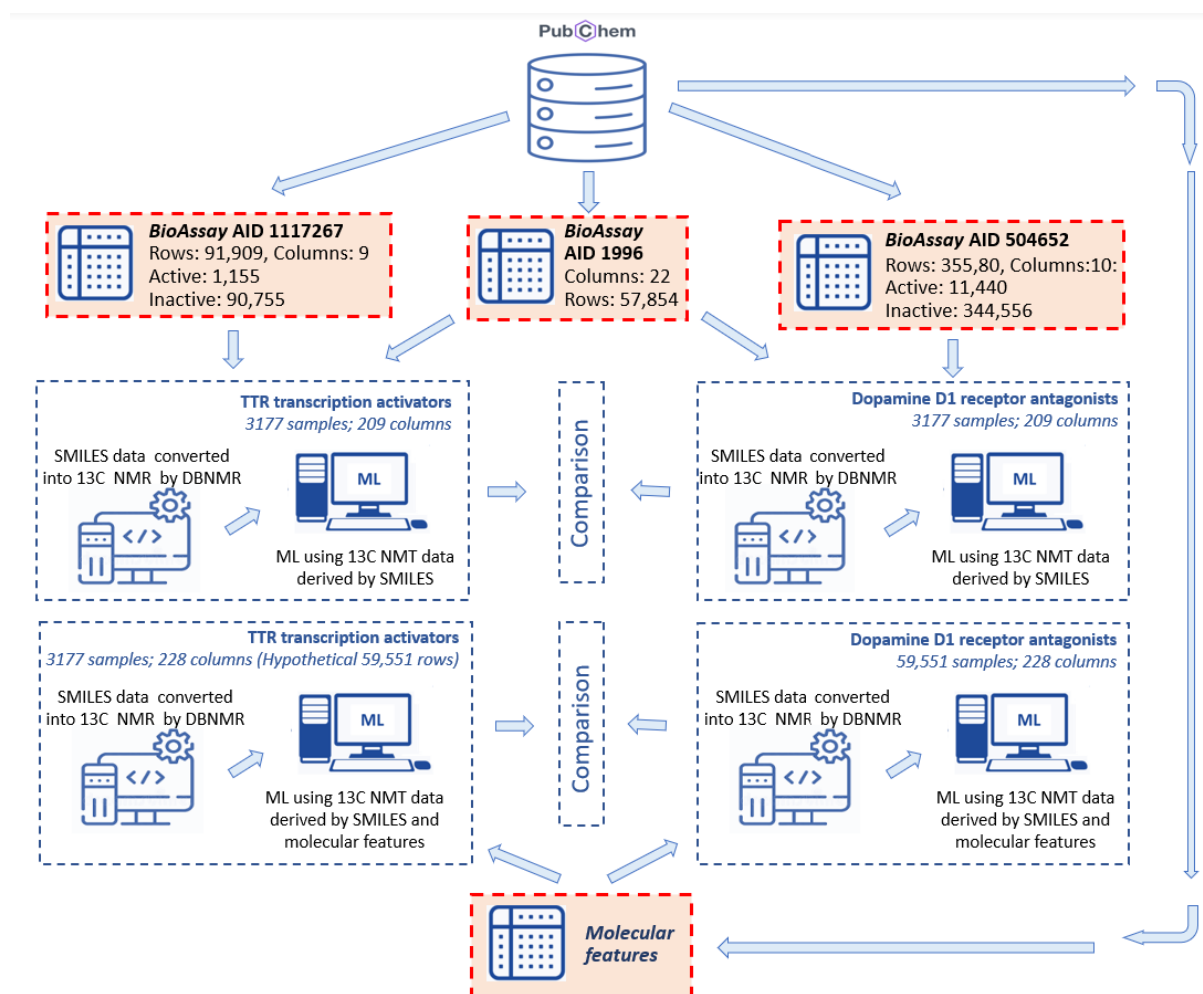


Figure 1. Methodology

Table 1. ML results obtained before scrutinising for overfitting. The TTR ML values marketed with \* hypothetical value calculated theoretically based on the percentage of increase of metrics for dopamine D1 receptor antagonists based on increase of the samples.

Case study & dataset	Train with 3,366 samples Test with 680 samples			Train with 27,756 samples Test with 5,466 samples		
	Accuracy [%]	Cross-val.	Tables	Accuracy [%]	Cross-val.	Tables
TTR & no PCA	<b>GBC</b>			61.82*	-	-
	56.8	0.651	ESM 1, 2			
TTR & with PCA	<b>GBC</b>			-	-	-
	56.2	0.739	ESM 3, 4			
	<b>GBC</b>					



<b>TTR &amp; no PCA &amp; PubChem mol. data</b>	67.1	0.683	ESM 13, 14	67.1*	-	-
<b>TTR &amp; with PCA &amp; PubChem mol. data</b>	<b>SVC</b>		ESM 15, 16	-	-	-
<b>D1 &amp; no PCA</b>	<b>SVC</b>		ESM5, 6	<b>SVC</b>		ESM9, 10
<b>D1 &amp; with PCA</b>	<b>SVC</b>		ESM7, 8	<b>SVC</b>		ESM11, 12
<b>D1 &amp; no PCA &amp; PubChem mol. data</b>	<b>RFC</b>		ESM 17, 18	<b>GBC</b>		ESM21, 22
<b>D1 &amp; with PCA &amp; PubChem mol. data</b>	<b>GBC</b>		EDM19, 20	<b>SVC</b>		ESM23, 24

Predicting the TTR transcription activator's capability of small biomolecule using the CID\_SID ML model achieved accuracy of 81.5%, precision of 94.6%, recall of 66.8%, F1-score of 78.3% and ROC of 81.5% with GBC at max\_depth=3 (Figure ESM7). The ML model was trained with 3,358 and tested with 680 samples. Regarding the CID\_SID ML model predicting the dopamine D1 receptor antagonists, the ML model has been already developed (14) obtaining accuracy of 80.2%, precision of 86.3, recall of 70.4%, F1-score of 77.6% and ROC of 79.9% trained with 19,438 and tested with 4,723 samples.

## Limitations

The dimensionality reduction with PCA was performed based on the suggested number of components based two methods: the first was based on the cumulative explained variance ratio, and the second employed Minka's MLE to estimate the number of dimensions (37). The number of the component for the different cases were, as follow:

- (i) 209 features of dataset with 3177 samples, used to predict TTR transcription activators, was dimensionality reduced to 186 features
- (ii) 209 features of dataset with 3177 samples, used to predict dopamine D1 receptor antagonists, was dimensionality reduced to 186 features
- (iii) 228 features of dataset with 3177 samples, used to predict TTR transcription activators was dimensionality reduced to 186 features

- (iv) 228 features of dataset with 3177 samples, used to predict dopamine D1 receptor antagonists was dimensionality reduced to 186 features
- (v) 228 features of dataset with 49,551 samples, 59,551 sample, used to predict dopamine D1 receptor antagonists was dimensionality reduced to 187 features.

However, the number of PCA components could be reduced by other technique, which were not explored in the study. For the explored variants, only (iv) Improved the accuracy. Since the time needed for training was not significant, the reduction of the time needed for ML was not taken into consideration.

Hyperparameter tuning was performed by Optuna. On the one hand, the number of studies were 5 and 10, but their increase is expected to bring better. On the other hand, there are other hyperparameter technique which can be explored in order to improve the performance of the ML models. The same is with the choice of classification estimators or balancing technique. In both cases there are room for more exploration in this direction, but the paper aim of the paper was to present the idea of the approach, the chosen techniques were sufficient for the presentation of the idea of the approach, however, there are endless options for exploration of the combination of the ML techniques.

The dataset used to predict TTR transcription activators contained insufficient number of samples. The number of samples was insufficient for the explored approach, however techniques, such as qHTS, which was used for the bioassays, has the potential to provide the necessary amount of data.

## Conclusion

The lower number of samples used for training and testing of the ML model to predict the human dopamine D1 receptor antagonists achieved lower results than the ML model trained and tested with the full sets of small biomolecules. This scalability dependence was used to calculate the hypothetical accuracy for predicting the TTR transcription activators. However, the big difference of the ML models` results for the small dataset of these two case studies implied that the ML approach is a case study dependent, so that the hypothetical accuracy is recommended to be tested with real data. Given that such data is not available, the exploration of the ML approach reminded open for exploration with other bioassays that have significant and sufficient number of samples. On the other hand, the addition of atomic features of the biomolecule for both bioassays improved the ML models except the variant with atomic features and a full dataset on human dopamine D1 receptor antagonists. It performed worse than the ML model with a reduced number of features. The hypothesis is that the model's complexity obstructs it from achieving better results.

The computational approaches developed beyond the main course of the paper, such as the CID\_SID ML model and IUPAC based approach offered a cost-effective and rapid way to gain early knowledge about potential side effects of drug candidates with respect to TTR transcription activators or dopamine D1 receptor antagonists.

Although the utilized <sup>13</sup>C NMR spectroscopy data is typically classical, the encoded into it information corresponds to the interaction of the quantum mechanical nature of matter and the light.

## Scientific Contribution

- A step forward toward development of universal model for predicting functionalities of small biomolecules based on NMR spectroscopy data through addition of molecular features that increased the ML model accuracy with 8%
- Developing a CID\_SID ML model for TTR transcription activators that can predict with 80.2% accuracy if a small biomolecule would cause a TTR transcription activation, that in turn could be useful for predicting of such a side effect.

### **Author Contributions**

MLI, NR, KN conceptualized the project and designed the methodology. MLI and NR wrote the code and processed the data. KN supervised the project. All authors were involved with the writing of the paper.

### **Data and Code Availability Statement**

The raw data used in the study is available through the PubChem portal:

<https://pubchem.ncbi.nlm.nih.gov/>

The code generated during the research is available on GitHub:

[https://github.com/articlesmli/13C\\_NMR\\_ML\\_model\\_TTR\\_D1.git](https://github.com/articlesmli/13C_NMR_ML_model_TTR_D1.git)

### **Conflicts of interest**

There are no conflicts to declare.

### **Acknowledgements**

MLI thanks UWL Vice-Chancellor's Scholarship scheme for their generous support. We sincerely thank to PubChem for providing access to their database. This article is dedicated to

## References

1. Jacobsen, N. E. NMR Spectroscopy Explained: Simplified Theory, Applications and Examples for Organic Chemistry and Structural Biology, **2007**, John Wiley & Sons, Inc., DOI: [10.1002/9780470173350](https://doi.org/10.1002/9780470173350)
2. Marion, D. An introduction to biological NMR spectroscopy. *Mol. Cel. Proteomics* **2013**, 12 (11), 3006-25, DOI: [10.1074/mcp.o113.030239](https://doi.org/10.1074/mcp.o113.030239)
3. Williamson, D.; Ponte, S.; Iglesias, I.; Tonge, N.; Cobas, C.; Kemsley, E. K. Chemical shift prediction in  $^{13}\text{C}$  NMR spectroscopy using ensembles of message passing neural networks (MPNNs). *J. Magn. Reson.* **2024**, 368, 107795, DOI: [10.1016/j.jmr.2024.107795](https://doi.org/10.1016/j.jmr.2024.107795)
4. Rull, H.; Fischer, M.; Kuhn, S. NMR shift prediction from small data quantities. *Jornal of Cheminform.* **2023**, 15, 114, DOI: [10.1186/s13321-023-00785-x](https://doi.org/10.1186/s13321-023-00785-x)
5. Cortés, I.; Cuadrado, C.; Hernández D. A.; Sarotti, A. M. Machine learning in computational NMR-aided structural elucidation. *Front. Nat. Prod.* **2023**, 2, 1122426, DOI: [10.3389/fntpr.2023.1122426](https://doi.org/10.3389/fntpr.2023.1122426)
6. Klukowski, P.; Riek, R.; Güntert, P. Time-optimized protein NMR assignment with an integrative deep learning approach using AlphaFold and chemical shift prediction. *Sci. Adv.* **2023**, 9, eadi9323. DOI: [10.1126/sciadv.adi9323](https://doi.org/10.1126/sciadv.adi9323)
7. Bret, C. L. (2000). A General  $^{13}\text{C}$  NMR Spectrum Predictor Using Data Mining Techniques. *SAR QSAR Environ. Res.* **2000**, 11(3–4), 211–234, DOI: [10.1080/10629360008033232](https://doi.org/10.1080/10629360008033232)
8. Jonas, E.; Kuhn, S.; Schlörer, N; Prediction of chemical shift in NMR: A review. *Magn Reson Chem.* **2022**, 60(11), 1021-1031. DOI: [10.1002/mrc.5234](https://doi.org/10.1002/mrc.5234)
9. Jonas, E.; Kuhn, S.; Schlörer, N. Prediction of chemical shift in NMR: A review, *Magn. Reson. Chem.* **2022**, 60(11), 1021, DOI: [10.1002/mrc.5234](https://doi.org/10.1002/mrc.5234)
10. Xin, D.; Sader, C., A.; Chaudhary, O.; Jones, P.; Wagner, K.; Tautermann, K., S; et al Development of a  $^{13}\text{C}$  NMR Chemical Shift Prediction Procedure Using B3LYP/cc-pVDZ and Empirically Derived Systematic Error Correction Terms: A Computational Small Molecule Structure Elucidation Method *J. Org. Chem.* **2017**, 82 (10), 5135-5145 DOI: [10.1021/acs.joc.7b00321](https://doi.org/10.1021/acs.joc.7b00321)
11. CASPER Reilly, D., Wren, C., Giles, S., Cunningham, L., & Hargreaves, P. (2016). *CASPER: Computer Assisted Search Prioritisation and Environmental Response Application*.

12. Emerenciano V., P.; Diego, D., G.; Ferreira M., J., P.; Scotti, M., T.; Comasseto, J., V.; Rodrigues, G., V. Computer-aided prediction of  $^{125}\text{Te}$  and  $^{13}\text{C}$  NMR chemical shifts of diorgano tellurides. *J. Braz. Chem. Soc.* **2007**, 18(6), 1183-1188. DOI: [10.1590/S0103-50532007000600012](https://doi.org/10.1590/S0103-50532007000600012)

13 NMRDB <https://nmrshiftdb.nmr.uni-koeln.de/> Accessed May 18, 2025.

14. Ivanova, M., L.; Russo, N.; Nikolic, K. Leveraging  $^{13}\text{C}$  NMR spectroscopic data derived from SMILES to predict the functionality of small biomolecules by machine learning: a case study on human Dopamine D1 receptor antagonists, *ArXiv*, Preprint at DOI: [10.48550/arXiv.2501.14044](https://doi.org/10.48550/arXiv.2501.14044)

15. National Center for Biotechnology Information. PubChem Bioassay Record for AID 504652, Antagonist of Human D 1 Dopamine Receptor: qHTS, Source: National Center for Advancing Translational Sciences (NCATS). <https://pubchem.ncbi.nlm.nih.gov/bioassay/504652>. Accessed May 18, 2025.

16. National Institutes of Health, PubChem <https://pubchem.ncbi.nlm.nih.gov/> Accessed May 18, 2025.

17. National Center for Biotechnology Information. PubChem Bioassay Record for AID 1117267, Source: The Scripps Research Institute Molecular Screening Center. <https://pubchem.ncbi.nlm.nih.gov/bioassay/1117267>. Accessed Apr. 20, 2025.

18. Buxbaum, J.N.; Reixach, N. Transthyretin: The Servant of Many Masters. *Cell Mol Life Sci.* **2009**, 66(19), 3095-101, DOI: [10.1007/s00018-009-0109-0](https://doi.org/10.1007/s00018-009-0109-0)

19. Ueda, M. Transthyretin: Its Function and Amyloid Formation, *Neurochem. Int.* **2022**, 155, 105313, DOI: [10.1016/j.neuint.2022.105313](https://doi.org/10.1016/j.neuint.2022.105313)

20. Liz, M., A.; Coelho, T.; Bellotti, V.; Fernandez-Arias, M., I; Mallaina, P.; Obici, L. A Narrative Review of the Role of Transthyretin in Health and Disease. *Neurol Ther.* **2020**, 9(2), 395-402, DOI: [10.1007/s40120-020-00217-0](https://doi.org/10.1007/s40120-020-00217-0)

21. Nikitin, D.; Wasfy, J., H; Winn, A., N.; Raymond, F.; Shah, K., K.; Kim, S. et al. The effectiveness and value of disease-modifying therapies for transthyretin amyloid cardiomyopathy: A summary from the Institute for Clinical and Economic Review's Midwest Comparative Effectiveness Public Advisory Council, *J. Manag. Care Spec. Pharm.* **2025**, 31(3), 323-8, DOI: <https://www.jmcp.org/doi/abs/10.18553/jmcp.2025.31.3.323>

22. Fleming CE, Saraiva MJ, Sousa MM. Transthyretin enhances nerve regeneration. *J Neurochem.* **2007**, 103, 831–839. doi: [10.1111/j.1471-4159.2007.04828.x](https://doi.org/10.1111/j.1471-4159.2007.04828.x)

23. Fleming, C.E.; Mar, F.M.; Franquinho, F.; Saraiva, M., J.; Sousa, M., M. Transthyretin internalization by sensory neurons is megalin mediated and necessary for its neurotogenic activity, *J Neurosci.* **2009**, 29, 3220–3232. DOI: [10.1523/JNEUROSCI.6012-08.2009](https://doi.org/10.1523/JNEUROSCI.6012-08.2009)

24. Rios, X.; Gómez-Vallejo, V.; Martín, A.; Cossío, U.; Morcillo, M. A.; Alemi, M. *et al.* Radiochemical examination of transthyretin (TTR) brain penetration assisted by iododiflunisal, a TTR tetramer stabilizer and a new candidate drug for AD. *Sci Rep* **2019**, *9*, 13672, DOI: [10.1038/s41598-019-50071-w](https://doi.org/10.1038/s41598-019-50071-w)
25. Nunes, A., F.; Saraiva M. J.; Sousa M., M. Transthyretin knockouts are a new mouse model for increased neuropeptide Y, *FASEB J* **2007**, *20*(1), 166-168, DOI: [10.1096/fj.05-4106fje](https://doi.org/10.1096/fj.05-4106fje)
26. Magalhães, J.; Eira, J.; Liz, M., A. The role of transthyretin in cell biology: impact on human pathophysiology. *Cell Mol Life Sci.* **2021**, *78*(17-18), 6105-6117, DOI: [10.1007/s00018-021-03899-3](https://doi.org/10.1007/s00018-021-03899-3)
27. Ivanova, M., L.; Russo, N.; Djaid, N.; Nikolic, K. Application of machine learning for predicting G9a inhibitors, *Digital Discovery*, **2024**, *3*(10), 2010-2018, DOI: [10.1039/D4DD00101J](https://doi.org/10.1039/D4DD00101J)
28. Ivanova, M., L.; Russo, N.; Djaid, N.; Nikolic, K. Targeting Neurodegeneration: Three Machine Learning Methods for Discovering G9a Inhibitors Using PubChem and Scikit-Learn, *ArXiv*, **2025**, Preprint at DOI: [10.48550/arXiv.2503.16214](https://doi.org/10.48550/arXiv.2503.16214)
29. Ertl, P.; Rohde, B.; Selzer, P. Fast calculation of molecular polar surface area as a sum of fragment-based contributions and its application to the prediction of drug transport properties. *J Med Chem.* **2000**, *43*(20), 3714-7, DOI: [10.1021/jm000942e](https://doi.org/10.1021/jm000942e)
30. Cheng, T.; Zhao, Y.; Li, X.; Lin, F.; Xu, Y.; Zhang, X. Computation of octanol-water partition coefficients by guiding an additive model with knowledge, *J. Chem. Inf. Model.* **2007**, *47*(6), 2140-8, DOI: [10.1021/ci700257y](https://doi.org/10.1021/ci700257y)
31. van der Veen, A., M., H.; Meija, J.; Possolo, A., A.; Hibbert, D., B. Interpretation and use of standard atomic weights (IUPAC Technical Report), *Pure Appl. Chem.* **2021**, *93* (5), 629-646, DOI: [10.1515/pac-2017-1002](https://doi.org/10.1515/pac-2017-1002)
32. Ivanova, M., L.; Russo, N.; Nikolic, K. Hierarchical Functional Group Ranking via IUPAC Name Analysis for Drug Discovery: A Case Study on TDP1 Inhibitors, *ArXiv*, **2025**, Preprint at DOI: [10.48550/arXiv.2503.05591](https://doi.org/10.48550/arXiv.2503.05591)
33. International Union of Pure and Applied Chemistry, <https://iupac.org/> Accessed May 18, 2025.
34. Ivanova, M., L.; Russo, N.; Nikolic, K. Predicting novel pharmacological activities of compounds using PubChem IDs and machine learning (CID-SID ML model), *ArXiv*, **2025**, Preprint at DOI: [10.48550/arXiv.2501.02154](https://doi.org/10.48550/arXiv.2501.02154)



35. Kim, S.; Thiessen, P., A; , Bolton, E., E; Chen, J.; Fu, G. Gindulyte, A. et al. PubChem Substance and Compound databases, *Nucleic Acids Res.* **2016**, *44*, D1202-13, DOI: [10.1093/nar/gkv951](https://doi.org/10.1093/nar/gkv951)

36. National Center for Biotechnology Information. PubChem Bioassay Record for AID 1996, Aqueous Solubility from MLSMR Stock Solutions, Source: Burnham Center for Chemical Genomics. <https://pubchem.ncbi.nlm.nih.gov/bioassay/1996>. Accessed May 18, 2025.

37. scikit-learn. PCA. <https://scikit-learn.org/stable/modules/generated/sklearn.decomposition.PCA.html> Accessed May 18, 2025.

## Supplementary materials

### Tables

Table ESM1. Results of the ML metrics regarding the TTR case performed without dimensionality reduction.

1.Algorithm	2.Accuracy	3.Precision	4.Recall	5.F1	6.ROC
GradientBoost	0.568	0.592	0.435	0.502	0.568
SVM	0.560	0.596	0.374	0.459	0.560
K-nearest	0.550	0.596	0.312	0.409	0.550
RandomForest	0.538	0.691	0.138	0.230	0.538
Decision	0.521	0.527	0.403	0.457	0.521

Table ESM2. A five-fold cross-validation for the TTR case performed without dimensionality reduction.

1.Algorithm	2.Mean CV Score	3.Standard Deviation	4.List of CV Scores
RandomForest	0.8637	0.0612	[0.7923, 0.8039, 0.8559, 0.9465, 0.9198]
Decision	0.7573	0.0352	[0.7285, 0.7221, 0.737, 0.8083, 0.7905]
SVM	0.7288	0.0307	[0.6899, 0.7043, 0.7311, 0.7786, 0.74]
K-nearest	0.6875	0.0431	[0.6543, 0.6256, 0.6895, 0.7355, 0.7325]
GradientBoost	0.6509	0.0195	[0.6365, 0.6627, 0.6196, 0.6686, 0.6672]

Table ESM3. Results of the ML metrics regarding the TTR case performed with dimensionality reduction with PCA

1.Algorithm	2.Accuracy	3.Precision	4.Recall	5.F1	6.ROC
GradientBoost	0.584	0.654	0.356	0.461	0.584
SVM	0.572	0.626	0.359	0.456	0.572
Decision	0.563	0.597	0.388	0.471	0.563
K-nearest	0.534	0.551	0.368	0.441	0.534
RandomForest	0.531	0.769	0.088	0.158	0.531

Table ESM4. A five-fold cross-validation for the TTR case performed with dimensionality reduction achieved with PCA.

1.Algorithm	2.Mean CV Score	3.Standard Deviation	4.List of CV Scores
RandomForest	0.8833	0.0568	[0.8145, 0.8262, 0.8826, 0.9554, 0.9376]
Decision	0.7834	0.0361	[0.7329, 0.7533, 0.786, 0.8187, 0.8262]
GradientBoost	0.7448	0.0337	[0.6988, 0.7147, 0.7489, 0.786, 0.7756]
SVM	0.7374	0.0391	[0.7122, 0.6895, 0.7207, 0.7964, 0.7682]
K-nearest	0.6661	0.0458	[0.6128, 0.6196, 0.6627, 0.7266, 0.7088]

Table ESM5. Results of the ML metrics regarding the dopamine D1 receptor case performed without dimensionality reduction.

1.Algorithm	2.Accuracy	3.Precision	4.Recall	5.F1	6.ROC
SVM	0.657	0.703	0.544	0.614	0.657
GradientBoost	0.650	0.692	0.541	0.607	0.650
RandomForest	0.601	0.822	0.259	0.394	0.601
Decision	0.571	0.588	0.471	0.523	0.571
K-nearest	0.512	0.520	0.309	0.387	0.512

Table ESM6. A five-fold cross-validation for the dopamine D1 receptor case performed without dimensionality reduction.

1.Algorithm	2.Mean CV Score	3.Standard Deviation	4.List of CV Scores
RandomForest	0.8817	0.0495	[0.847, 0.8083, 0.8856, 0.9242, 0.9435]
Decision	0.7809	0.0334	[0.7533, 0.7519, 0.7652, 0.7935, 0.8408]
SVM	0.7753	0.0291	[0.7504, 0.7385, 0.7816, 0.7845, 0.8214]
GradientBoost	0.7045	0.0217	[0.6805, 0.6805, 0.7058, 0.7207, 0.7351]
K-nearest	0.6938	0.0287	[0.6746, 0.6612, 0.6776, 0.7207, 0.7351]

Table ESM7. Results of the ML metrics regarding the dopamine D1 receptor case performed with dimensionality reduction.

1.Algorithm	2.Accuracy	3.Precision	4.Recall	5.F1	6.ROC
SVM	0.647	0.692	0.529	0.600	0.647
GradientBoost	0.600	0.705	0.344	0.462	0.600
Decision	0.537	0.559	0.350	0.430	0.537
RandomForest	0.534	0.677	0.129	0.217	0.534
K-nearest	0.519	0.532	0.321	0.400	0.519

Table ESM8 A five-fold cross-validation for the dopamine D1 receptor case performed and dimensionality reduction with PCA

1.Algorithm	2.Mean CV Score	3.Standard Deviation	4.List of CV Scores
RandomForest	0.8764	0.0565	[0.8306, 0.7994, 0.8767, 0.9227, 0.9524]
Decision	0.7854	0.0537	[0.7801, 0.7266, 0.7296, 0.8276, 0.8631]
GradientBoost	0.7747	0.0522	[0.7281, 0.7073, 0.7831, 0.8024, 0.8527]
SVM	0.7485	0.0362	[0.7221, 0.6969, 0.7637, 0.7578, 0.8021]
K-nearest	0.6917	0.0226	[0.6672, 0.6657, 0.6969, 0.7043, 0.7247]

Table ESM9 Metrics results of ML with a full dataset of <sup>13</sup>CNMR and molecular features for predicting dopamine D1 receptor antagonists

1.Algorithm	2.Accuracy	3.Precision	4.Recall	5.F1	6.ROC
SVM	0.715	0.774	0.606	0.680	0.715
XGBoost	0.688	0.737	0.587	0.653	0.688
RandomForest	0.653	0.792	0.416	0.546	0.653
GradientBoost	0.650	0.674	0.582	0.625	0.650
K-nearest	0.612	0.671	0.441	0.532	0.612
Decision	0.578	0.596	0.483	0.534	0.578

Table ESM10. Five-fold cross-validation of ML based on a full dataset with <sup>13</sup>CNMR and molecular features for predicting dopamine D1 receptor antagonists

1.Algorithm	2.Mean CV Score	3.Standard Deviation	4.List of CV Scores
SVM	0.7487	0.0030	[0.7508, 0.7461, 0.7536, 0.7472, 0.7461]
XGBoost	0.7207	0.0054	[0.7252, 0.7144, 0.7236, 0.7265, 0.7141]
RandomForest	0.7073	0.0021	[0.7065, 0.7084, 0.7102, 0.7073, 0.704]
GradientBoost	0.6885	0.0048	[0.6925, 0.6872, 0.6861, 0.6954, 0.6817]
K-nearest	0.6429	0.0059	[0.6509, 0.6356, 0.6476, 0.6432, 0.637]
Decision	0.6012	0.0065	[0.6096, 0.6059, 0.5939, 0.6034, 0.5933]

Table ESM11. Metric results of ML with a full dataset of 13CNMR and molecular feature and dimensionality reduced by PCA for predicting dopamine D1 receptor antagonists

1.Algorithm	2.Accuracy	3.Precision	4.Recall	5.F1	6.ROC
SVM	0.642	0.696	0.506	0.586	0.642
RandomForest	0.619	0.704	0.411	0.519	0.619
GradientBoost	0.619	0.645	0.530	0.582	0.619
XGBoost	0.615	0.659	0.478	0.554	0.615
K-nearest	0.580	0.612	0.438	0.511	0.580
Decision	0.544	0.555	0.444	0.493	0.544

Table ESM12. Five-fold cross-validation of ML based on a full dataset with 13CNMR and molecular features, reduced by PCA for predicting dopamine D1 receptor antagonists

1.Algorithm	2.Mean CV Score	3.Standard Deviation	4.List of CV Scores
SVM	0.6830	0.0052	[0.6881, 0.6808, 0.6782, 0.6903, 0.6778]
RandomForest	0.6713	0.0072	[0.6736, 0.6601, 0.6753, 0.6809, 0.6667]
GradientBoost	0.6663	0.0074	[0.6775, 0.659, 0.6654, 0.6718, 0.6581]
XGBoost	0.6616	0.0040	[0.6676, 0.6595, 0.6561, 0.6645, 0.6604]
K-nearest	0.6205	0.0043	[0.6239, 0.6147, 0.6158, 0.6239, 0.6242]
Decision	0.5780	0.0094	[0.5878, 0.5752, 0.5856, 0.5801, 0.5615]

Table ESM13. Metric results of ML with a full dataset of <sup>13</sup>CNMR and molecular feature and dimensionality reduced by PCA for predicting dopamine D1 receptor antagonists.

1.Algorithm	2.Accuracy	3.Precision	4.Recall	5.F1	6.ROC
GradientBoost	0.671	0.740	0.526	0.615	0.671
RandomForest	0.656	0.794	0.421	0.550	0.656
SVM	0.604	0.671	0.409	0.508	0.604
Decision	0.596	0.638	0.441	0.522	0.596
K-nearest	0.547	0.562	0.429	0.487	0.547

Table ESM14. A five-fold cross-validation for predicting TTR transcription antagonists based on a dataset with added molecular features.

1.Algorithm	2.Mean CV Score	3.Standard Deviation	4.List of CV Scores
RandomForest	0.8899	0.0369	[0.8556, 0.8507, 0.8756, 0.9331, 0.9347]
Decision	0.8032	0.0429	[0.75, 0.7792, 0.7792, 0.86, 0.8476]
SVM	0.7245	0.0272	[0.6879, 0.7045, 0.7201, 0.7496, 0.7605]
GradientBoost	0.6931	0.0186	[0.6599, 0.6874, 0.6983, 0.7123, 0.7076]
K-nearest	0.6645	0.0499	[0.6335, 0.6112, 0.6345, 0.7465, 0.6967]

Table ESM15. ML metric results based on a full dataset with <sup>13</sup>C NMR, and molecular feature and dimensionality reduced by PCA for predicting TTR transcription activators.

1.Algorithm	2.Accuracy	3.Precision	4.Recall	5.F1	6.ROC
SVM	0.650	0.707	0.512	0.594	0.650
GradientBoost	0.604	0.625	0.521	0.568	0.604
K-nearest	0.534	0.536	0.503	0.519	0.534
Decision	0.519	0.528	0.359	0.427	0.519
RandomForest	0.519	0.528	0.359	0.427	0.519

Table ESM16. A five-fold cross-validation for predicting TTR transcription activators based on a dataset with <sup>13</sup>C NMR and molecular feature and dimensionality reduced by PCA.



1.Algorithm	2.Mean CV Score	3.Standard Deviation	4.List of CV Scores
GradientBoost	0.7172	0.0127	[0.7061, 0.7023, 0.7138, 0.7352, 0.7286]
RandomForest	0.7146	0.0099	[0.7126, 0.7072, 0.7023, 0.7303, 0.7204]
SVM	0.6952	0.0093	[0.6847, 0.6891, 0.6908, 0.7007, 0.7105]
K-nearest	0.6449	0.0203	[0.6338, 0.6382, 0.6266, 0.6414, 0.6842]
Decision	0.6090	0.0092	[0.5944, 0.6102, 0.6168, 0.6036, 0.6201]

Table ESM17. ML metric results based on a reduced dataset of 13CNMR and molecular features for predicting dopamine D1 receptor antagonists.

1.Algorithm	2.Accuracy	3.Precision	4.Recall	5.F1	6.ROC
GradientBoost	0.762	0.850	0.635	0.727	0.762
RandomForest	0.749	0.889	0.568	0.693	0.749
SVM	0.691	0.773	0.541	0.637	0.691
Decision	0.687	0.738	0.579	0.649	0.687
K-nearest	0.576	0.620	0.394	0.482	0.576

Table ESM18. Five-fold cross-validation of ML based on a reduced dataset with 13CNMR and molecular features for predicting dopamine D1 receptor antagonists

1.Algorithm	2.Mean CV Score	3.Standard Deviation	4.List of CV Scores
RandomForest	0.9300	0.0180	[0.9145, 0.9129, 0.9191, 0.9487, 0.9548]
Decision	0.8541	0.0216	[0.8336, 0.8305, 0.8476, 0.8756, 0.8832]
SVM	0.8208	0.0201	[0.7978, 0.7963, 0.8274, 0.8445, 0.838]
GradientBoost	0.7828	0.0053	[0.7854, 0.7823, 0.7776, 0.7916, 0.7773]
K-nearest	0.7231	0.0496	[0.6594, 0.6765, 0.7232, 0.776, 0.7804]

Table ESM19. ML metric results based on a reduced dataset of 13CNMR and molecular features for predicting dopamine D1 receptor antagonists.

1.Algorithm	2.Accuracy	3.Precision	4.Recall	5.F1	6.ROC
GradientBoost	0.704	0.833	0.512	0.634	0.704
SVM	0.687	0.759	0.547	0.636	0.687
RandomForest	0.672	0.868	0.406	0.553	0.672
Decision	0.585	0.626	0.424	0.505	0.585
K-nearest	0.576	0.621	0.391	0.480	0.576

Table ESM20. Five-fold cross-validation of ML based on a reduced dataset with <sup>13</sup>CNMR and molecular features, dimensionality reduced by PCA for predicting dopamine D1 receptor antagonists.

1.Algorithm	2.Mean CV Score	3.Standard Deviation	4.List of CV Scores
RandomForest	0.9031	0.0378	[0.8618, 0.8692, 0.8886, 0.9421, 0.9539]
GradientBoost	0.8347	0.0264	[0.7994, 0.8187, 0.8247, 0.8648, 0.8661]
Decision	0.8220	0.0352	[0.7771, 0.789, 0.8217, 0.8559, 0.8661]
SVM	0.8121	0.0240	[0.7845, 0.7979, 0.7994, 0.8276, 0.8512]
K-nearest	0.7307	0.0522	[0.6835, 0.6761, 0.7073, 0.7979, 0.7887]

Table ESM21. ML metric results based on a full dataset of <sup>13</sup>CNMR and molecular features for predicting dopamine D1 receptor antagonists

1.Algorithm	2.Accuracy	3.Precision	4.Recall	5.F1	6.ROC
GradientBoost	0.758	0.842	0.636	0.724	0.758
RandomForest	0.756	0.872	0.600	0.711	0.756
SVM	0.747	0.822	0.631	0.714	0.747
Decision	0.687	0.715	0.621	0.665	0.687
K-nearest	0.615	0.657	0.483	0.556	0.615

Table ESM22. Five-fold cross-validation of ML based on a full dataset with <sup>13</sup>CNMR and molecular features for predicting dopamine D1 receptor antagonists

1.Algorithm	2.Mean CV Score	3.Standard Deviation	4.List of CV Scores
RandomForest	0.8878	0.0469	[0.8475, 0.8473, 0.8547, 0.9362, 0.9532]
Decision	0.8085	0.0400	[0.7715, 0.7781, 0.7783, 0.8521, 0.8623]
SVM	0.8007	0.0210	[0.7785, 0.7799, 0.7946, 0.8218, 0.8288]
GradientBoost	0.7607	0.0039	[0.7599, 0.7548, 0.7636, 0.7589, 0.7662]
K-nearest	0.7104	0.0391	[0.6742, 0.6812, 0.6804, 0.7599, 0.7564]

Table ESM23. Metrics results of ML with a full dataset of 13CNMR and molecular features and dimensionality reduced by PCA for predicting dopamine D1 receptor antagonists

1.Algorithm	2.Accuracy	3.Precision	4.Recall	5.F1	6.ROC
SVM	0.743	0.820	0.623	0.708	0.743
GradientBoost	0.739	0.809	0.624	0.705	0.739
RandomForest	0.719	0.847	0.534	0.655	0.719
Decision	0.657	0.689	0.572	0.625	0.657
K-nearest	0.620	0.662	0.491	0.564	0.620

Table ESM24. Five-fold cross-validation of ML based on a full dataset with 13CNMR and molecular feature and dimensionality reduced by PCA for predicting dopamine D1 receptor antagonists

1.Algorithm	2.Mean CV Score	3.Standard Deviation	4.List of CV Scores
RandomForest	0.8701	0.0509	[0.8277, 0.8249, 0.8337, 0.925, 0.9393]
SVM	0.7931	0.0173	[0.7748, 0.7758, 0.7904, 0.804, 0.8204]
Decision	0.7840	0.0447	[0.746, 0.7482, 0.7489, 0.8306, 0.8463]
GradientBoost	0.7512	0.0052	[0.7474, 0.7439, 0.7538, 0.7521, 0.7589]
K-nearest	0.7056	0.0382	[0.6714, 0.6734, 0.679, 0.7472, 0.7571]

Figures

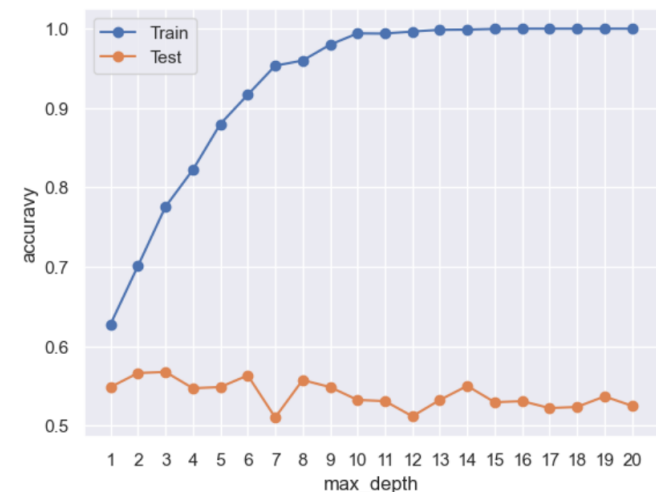


Figure ESM1. Tracing the deviation between train and test accuracies for the TTR case without dimensionality reduction

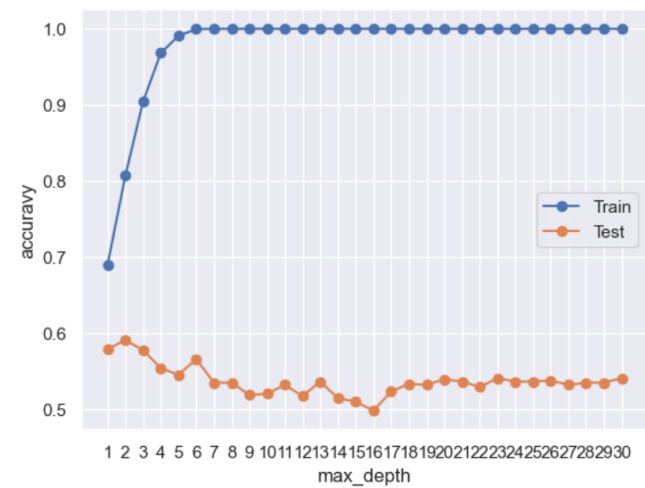


Figure ESM2. Tracing the deviation between train and test accuracies for the TTR case without dimensionality reduction

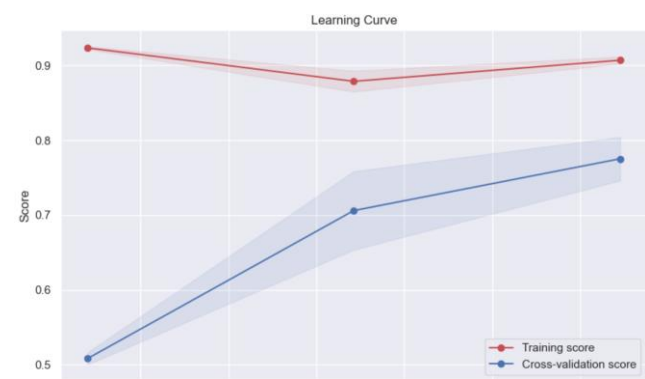


Figure 3. Learning curve dopamine D1 receptor case without dimentionality reduction

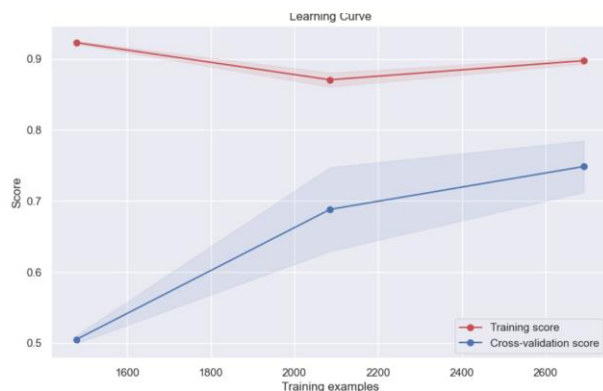


Figure 4. Learning curve dopamine D1 receptor case with dimensionality reduction

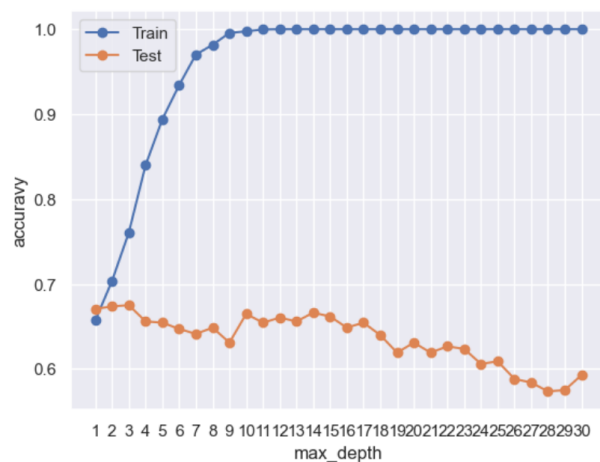


Figure ESM5. Tracing the deviation between train and test accuracies for the TTR case with molecular features added without dimensionality reduction

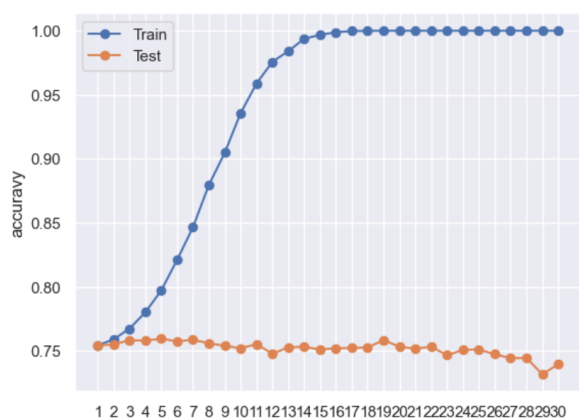


Figure ESM6. Tracing the deviation between train and test accuracies for the dopamine D1 receptor antagonist and molecular features case without dimensionality reduction

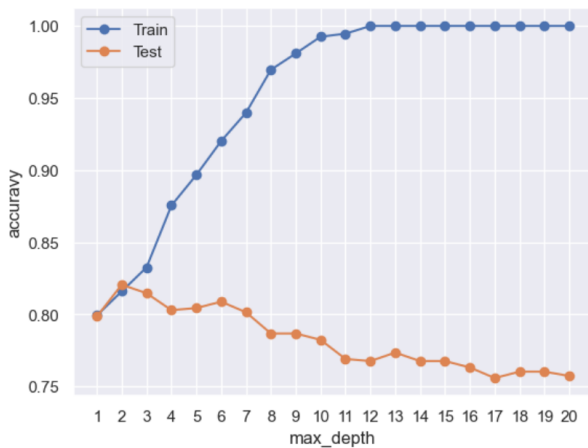


Figure ESM7. Tracing the deviation between train and test accuracies for the CID\_SID ML model based on TTR transcription activator dataset

